The active conformation of human glucokinase is not altered by allosteric activators

Pierre Petit,[a] Mathias Antoine,[b] Gilles Ferry,[b] Jean A. Boutin,[b]* Amandine Lagarde,[c] Laure Gluais,[c] Renaud Vincentelli[c] and Laurent Vuillard[a]*

[a]BioXtal, PX Unit, c/o AFMB, UMR 6098, Case 932, 163 Avenue de Luminy, 13288 Marseille CEDEX 09, France, [b]Biotechnologies, Pharmacologie Moléculaire et Cellulaire, Institut de Recherches Servier, 125 Chemin de Ronde, 78290 Croissy-sur-Seine, France, and [c]AFMB, UMR 6098, Case 932, 63 Avenue de Luminy, 13288 Marseille CEDEX 09, France

Correspondence e-mail:
jean.boutin@fr.netgrs.com,
lvuillard@bioxtal.com

Glucokinase (GK) catalyses the formation of glucose 6-phosphate from glucose and ATP. A specific feature of GK amongst hexokinases is that it can cycle between active and inactive conformations as a function of glucose concentration, resulting in a unique positive kinetic cooperativity with glucose, which turns GK into a unique key sensor of glucose metabolism, notably in the pancreas. GK is a target of antidiabetic drugs aimed at the activation of GK activity, leading to insulin secretion. Here, the first structures of a GK–glucose complex without activator, of GK–glucose–AMP-PNP and of GK–glucose–AMP-PNP with a bound activator are reported. All these structures are extremely similar, thus demonstrating that binding of GK activators does not result in conformational changes of the active protein but in stabilization of the active form of GK.

1. Introduction

Glucokinase (GK; also called hexokinase IV; EC 2.7.1.2), one of the four mammalian hexokinase isoenzymes, is the main enzyme responsible for glucose phosphorylation in hepatocytes and pancreatic islet beta cells (Agius, 2008). GK has different properties to other hexokinases: firstly, it does not display product inhibition by glucose 6-phosphate, and secondly, it possesses a much higher K_m for glucose than other hexokinases (5 mM versus 20–130 µM). This high K_m is a consequence of the existence in GK only of conformational changes between an inactive (open) and an active (closed) conformation triggered by variations in glucose concentration. A key point for the physiological function of GK is that the inflexion point of the activity versus glucose concentration curve is near the physiological concentration of glucose. A key element in this regulation is the C-terminal helix 13, as shown by mutations leading to diabetes and validated by in vitro studies (Vionnet et al., 1992). The existence of at least two conformations thus results in allosteric behaviour of GK even though it is a monomeric protein. Several groups, including ours, have recently reported on the mechanism of this transition and on the kinetics of conformational transitions associated with glucose binding using fluorescence and NMR spectroscopies (Antoine et al., 2009; Larion et al., 2010). These studies pointed towards the existence of conformational heterogeneity between apo and glucose-bound GK. However, in the absence of the corresponding structures (crystals of GK with either glucose alone or with an ATP analogue), the effects of activators on the structure of GK as well as the active conformation of GK remain unknown.

The metabolism of beta cells is directly coupled to the rate of glucose 6-phosphate production, which depends mostly on

GK activity (Matschinsky, 1990). The beta-cell glucose concentration is directly related to the plasma glucose concentration (owing to the high abundance of the Glut2 receptor), while the other substrate of GK (Mg-ATP) is present at nearly saturating concentration. Therefore, GK activity is directly coupled to the plasmatic concentration of glucose. This coupling between GK activity and plasma glucose concentration makes GK a glucose sensor for the secretion of insulin. Numerous mutations affect GK. Some of these GK mutations cause types of diabetes or affect the catalytic properties of GK, resulting in persistant hyper-insulinaemia–hypoglycaemia of infancy (Cuesta-Muñoz *et al.*, 2004; Vionnet *et al.*, 1992). This key position of GK in glucose regulation and in diabetes led to intensive efforts to develop new antidiabetic drugs targeting GK (Grimsby *et al.*, 2008; Matschinsky, 2009; Matschinsky *et al.*, 2011; Polakof, 2010). Amongst the strategies towards this end, the determination of the GK structure in both open and closed conformations was a major step in understanding the allosteric regulation of GK as well as the molecular mechanisms of GK activators (Antoine *et al.*, 2009; Molnes *et al.*, 2011). The structure of a 'super-open' (or relaxed), inactive, apo conformation (PDB entry 1v4t) was obtained in the absence of either glucose or activator (Kamata *et al.*, 2004). This open conformation possessed a distorted glucose-binding site with poor glucose affinity. A 'closed' conformation (PDB entry 1v4s) tightly bound to glucose and to an allosteric activator, *N*-thiazol-2-yl-2-amino-4-fluoro-5-(1-methylimidazol-2-yl)thiobenzamide (TAFMT), has also been described (Kamata *et al.*, 2004). Additional structures of GK bound to glucose and activators have been released (PDB entries 3h1v, 3imx, 3a0i, 3goi and 3fr0; Bebernitz *et al.*, 2009; Mitsuya *et al.*, 2009; Nishimura *et al.*, 2009; Takahashi *et al.*, 2009). The structures of PDB entries 3h1v, 3imx, 3a0i, 3goi and 3fr0 showed the same conformation and the same activator binding site as the TAFMT–GK–glucose structure. All of the GK structures deposited in the Protein Data Bank are summarized in Table 1. However, the following are not known: (i) the conformation of active GK in the presence of glucose and Mg-ATP and (ii) whether the active conformation of GK is altered by the binding of an allosteric activator.

In the present work, we describe the structures of glucose-bound active GK as well as of glucose-bound GK in the presence of the nonhydrolysable ATP analogue adenosine 5′-(β,γ-imino)triphosphate (AMP-PNP), in the presence of the allosteric activator TAFMT and in the presence of both AMP-PNP and TAFMT (PDB entries 3idh, 3fgu, 3f9m and 3id8, respectively). We demonstrate that the glucose-bound conformation is indeed the active conformation and that activators do not induce a change of conformation.

2. Material and methods

2.1. Materials

N-Thiazol-2-yl-2-amino-4-fluoro-5-(1-methylimidazol-2-yl)-thiobenzamide was discovered by Banyu Pharmaceutical and named TAFMT (Iino *et al.*, 2009; Mitsuya *et al.*, 2009). This

Table 1
Current glucokinase PDB entries and their ligands.

PDB entry	Ligands
1v4t	None
1v4s	Glucose, TAFMT {2-amino-4-fluoro-5-[(1-methyl-1*H*-imidazol-2-yl)sulfanyl]-*N*-(1,3-thiazol-2-yl)benzamide}
3a0i	Glucose, 3-[(4-fluorophenyl)sulfanyl]-*N*-(4-methyl-1,3-thiazol-2-yl)-6-[(4-methyl-4*H*-1,2,4-triazol-3-yl)sulfanyl]-pyridine-2-carboxamide
3goi	Glucose, 2-(methylamino)-*N*-(4-methyl-1,3-thiazol-2-yl)-5-[(4-methyl-4*H*-1,2,4-triazol-3-yl)sulfanyl]benzamide
3h1v	Glucose, 1-({5-[4-(methylsulfonyl)phenoxy]-2-pyridin- 2-yl-1*H*-benzimidazol-6-yl}methyl)pyrrolidine-2,5-dione
3imx	Glucose, (2*R*)-3-cyclopentyl-*N*-(5-methoxy[1,3]thiazolo[5,4-*b*]pyridin-2-yl)-2-{4-[(4-methylpiperazin-1-yl)sulfonyl]-phenyl}propanamide
3fr0	Glucose, 2-amino-*N*-(4-methyl-1,3-thiazol-2-yl)-5-[(4-methyl-4*H*-1,2,4-triazol-3-yl)sulfanyl]benzamide
3f9m	Glucose, TAFMT
3fgu	Glucose, AMP-PNP
3id8	Glucose, AMP-PNP, TAFMT
3idh	Glucose

compound was synthesized in-house and solubilized in DMSO to give a 20 m*M* solution. All chemicals were analytical grade.

2.2. Glucokinase expression and purification

Pancreatic human GK (Swiss-Prot P35557, isoform 1) was prepared as described previously (Antoine *et al.*, 2009). In brief, human GK isoform 1 (pancreatic) was cloned from residue 12 to the C-terminus in the pET28 vector. The construct also possessed an N-terminal hexahistidine tag followed by the TEV cleavage site ENLYFQG. Expression was obtained in *Escherichia coli* BL21 (DE3). Purification was performed on Ni–NTA followed by ion-exchange chromato-graphy on a HiTrap Q FF column and gel filtration on a Superdex 200 column. The enzyme purity was found to be >95% by SDS–PAGE and denaturing ESI-MS and its activity was >100 units mg^{-1}.

2.3. Crystallization

The crystallization samples were solutions of GK (at 6 or 10 mg ml^{-1}) in 20 m*M* HEPES, 50 m*M* KCl, 2 m*M* tris(2-carboxyethyl)phosphine (TCEP), 100 m*M* glucose, 5%(*w/v*) glycerol pH 7.5. When present, activators were diluted to a concentration of 80 µ*M* and added to the protein solution prior to concentration and AMP-PNP was added to a final concentration of 10 m*M* with the addition of 1 m*M* MgCl$_2$. Initial crystals were obtained under conditions similar to those described by Kamata *et al.* (2004) and showed the same unit-cell parameters. However, in our hands these crystals did not diffract well and grew very slowly. After extensive screening in a matrix of various PEGs buffered using HEPES pH 7.5, a different crystal form was obtained with space group $P2_12_12_1$. This crystal was further used for preliminary seeding experi-ments. All crystals used in this work were grown under the same conditions, *i.e.* at room temperature using hanging-drop vapour diffusion in Linbro plates. 2 µl protein solution was mixed with 1 µl reservoir solution (32–38% PEG 4000 in 100 m*M* HEPES pH 7.5). After 3 d of equilibration, drops

Table 2
PDB references, diffraction data and refinement.

Values in parentheses are for the outer shell.

Structure	GK–Glc	GK–Glc–TAFMT	GK–Glc–AMP-PNP	GK–Glc–AMP-PNP–TAFMT
PDB entry	3idh	3f9m	3fgu	3id8
Unit-cell parameters (Å)	$a = 65.5$, $b = 82.0$, $c = 86.0$	$a = 65.7$, $b = 81.2$, $c = 85.6$	$a = 65.9$, $b = 82.1$, $c = 86.8$	$a = 67.0$, $b = 82.6$, $c = 86.8$
Space group	$P2_12_12_1$			
Resolution (Å)	2.14 (2.24–2.14)	1.5 (1.6–1.5)	2.15 (2.25–2.15)	2.4 (2.5–2.4)
Unique reflections	26185	69412	22231	18338
Completeness (%)	99.0 (98.6)	93.9 (85.4)	84.8 (73.1)	95.8 (91.5)
$\langle I/\sigma(I)\rangle$	16.9 (3.0)	18.9 (3.7)	17.2 (3.1)	16.8 (5.2)
Multiplicity	4.1 (3.0)	3.2 (3.2)	3.6 (2.2)	6.3 (6.5)
R_{merge} (%)	8.7 (40)	4.2 (45)	6.7 (27)	9.0 (42)
R_{free} (%)	22	22	25.5	27
R factor (%)	19.1	19	19.6	20
R.m.s.d. bond lengths (Å)	0.011	0.010	0.011	0.013
R.m.s.d. bond angles (°)	1.28	1.33	1.26	1.51
Average B, protein (Å^2)	24.4	16	24	33.2
Average B, Glc (Å^2)	12	12	14	20
Average B, TAFMT (Å^2)	NA	24	NA	36
Average B, AMP-PNP (Å^2)	NA	NA	25	28

were seeded with crushed crystals diluted in reservoir solution. Crystals appeared within 12 h in the presence of TAFMT and notably more slowly in its absence and grew to their final dimensions within 2 d (with TAFMT) or longer (without TAFMT). Crystals were obtained over a range (32–38%) of PEG concentrations and cooled under liquid nitrogen without need for further cryoprotection.

2.4. Data collection and structure resolution

Data sets were collected on the SLS PX6d beamline (Villigen, Switzerland) and were reduced using *XDS* (Kabsch, 2010). In order to avoid any bias on the densities of the ligands, the following procedure was used for molecular replacement and structure refinement. Firstly, molecular replacement was performed using the program *MOLREP* (Vagin & Teplyakov, 2010). As a model, we used the structure 1v4s (Kamata *et al.*, 2004), from which we removed all ligands or bound waters. This was followed by refinement omitting all ligands using *REFMAC* (Murshudov *et al.*, 2011). After several refinement cycles, water molecules were built iteratively by *ARP/wARP* (Perrakis *et al.*, 2001). At this stage, the densities of the ligands were clearly visible and were then refined. Further refinement using TLS was also performed (Painter & Merritt, 2006). Crystallographic parameters and PDB references are presented in Table 2. Figures were drawn using *PyMOL*.

3. Results and discussion

3.1. General

The present report is the first to report the structure of a binary complex between GK and glucose. It is also the first to report the structure of an active GK in the presence of both glucose and the ATP analogue AMP-PNP. Finally, a ternary

complex comprising glucose, AMP-PNP and TAFMT with GK in an active conformation is also presented here for the first time.

The first obvious observation is that these new four structures are all similar to those published by Kamata and coworkers (Iino *et al.*, 2009; Kamata *et al.*, 2004; Mitsuya *et al.*, 2009; Nishimura *et al.*, 2009; Takahashi *et al.*, 2009), with GK bound to both glucose and activator. This is illustrated by the low r.m.s. deviations (in backbone positions) between our structures and the published structure of glucose-bound GK (PDB entry 1v4s): for the glucose/TAFMT complex the r.m.s. deviation is 0.70 Å, for the glucose/TAFMT/AMP-PNP complex the r.m.s. deviation is 0.61 Å, for the glucose complex the r.m.s. deviation is 0.73 Å and for the glucose/AMP-PNP complex the r.m.s. deviation is 0.73 Å. This common structure is indeed the active conformation of GK as it is also the structure obtained in the present work for the ternary complex GK–AMP-PNP–glucose. Simulated-annealing OMIT maps (SAOM; 3σ) showed density for both glucose (Fig. 1*a*) and TAFMT (Fig. 1*b*) in the 3f9m structure. A discontinuous density (adenine–ribose–phosphate) was observed in the SAOM (3σ) for AMP-PNP (Fig. 1*c*). To avoid possible bias, Fig. 1(*c*) shows a map calculated with the same resolution (2.15 Å) as those of the cocrystals with or without AMP-PNP (PDB entries 3idh and 3fgu, respectively). This discontinuous density belongs to AMP-PNP for the following reasons. Firstly, no density corresponding to the adenine or ribose molecules is visible in the SAOM from structures without AMP-PNP and furthermore these limited densities (attributed to water molecules) are apparent at the position of the strong density of the phosphate groups in the structures obtained with AMP-PNP. Secondly, $F_o - F_c$ OMIT maps (3σ; Fig. 1*d*) calculated during a final refinement step performed without any nucleotide in the model showed well positioned continuous density for AMP-PNP. Finally, no negative density in the region corresponding to the position of the ribose was observed when AMP-PNP was finally positioned into the structure. In conclusion, this density can reasonably be attributed to AMP-PNP. The density observed in the SAOM around AMP-PNP is poorest around the ribose. This could be a consequence of greater thermal agitation because the ribose is well exposed to the solvent. Furthermore, the interactions of the ribose with GK are limited to two hydrogen bonds only (Gly225 and Ser411).

It is worth noticing that TAFMT has no effect on the conformation of active GK either globally or at the locations of the partners involved in catalysis. The absence of global changes is illustrated by the C$^\alpha$ r.m.s. deviations reported

above and the absence of any obvious effect on the molecule flexibility that would have an effect on the *B* factors. All the reactive partners of the active site remain in the same position in the presence or the absence of an allosteric activator (Fig. 2*a*, glucose only; Fig. 2*b*, glucose and AMP-PNP). Furthermore, the position of TAFMT is not modified when AMP-PNP is present. The residues described as interacting with TAFMT by Kamata and coworkers (Arg63, Tyr215, Met210, Tyr214, Val452 and Val455) remain in the same positions upon AMP-PNP binding (Fig. 3). TAFMT shares the same site as other activators described by Kamata and coworkers and other proprietary compounds studied by our team (unpublished results). Another activator/GK/glucose structure has been published (Efanov *et al.*, 2005) but without a PDB deposition. These data do not point to any obvious differences. It can be noted that the positions of the residues possibly involved in the binding of TAFMT remain almost the same whether TAFMT is present or absent. The only differ-ence is the orientation of Tyr215, which is shifted away from the binding pocket in the absence of TAFMT.

3.2. Description of the active site of GK

The catalytic site (Fig. 4*a*) follows a classic kinase layout (Johnson, 2009; Zhang, Yang *et al.*, 2009). In the ternary GK–glucose–AMP-PNP structure the γ-phosphate group is aligned with the 6-hydroxyl group from the glucose at a distance of 2.7 Å, where it is well positioned to react with the 6-hydroxyl of glucose. A distance of 2.5 Å was measured between the hydroxyl group of Asp205 and the 6-hydroxyl of the glucose. This strongly suggests that the Asp205 carboxylate is the general base catalyst that activates glucose by deprotonating the 6-hydroxyl group. This structural evidence supports the early kinetic work of Lange *et al.* (1991), which revealed a 500-fold decrease in activity upon the mutation of Asp105 to alanine. The released proton would then shuttle
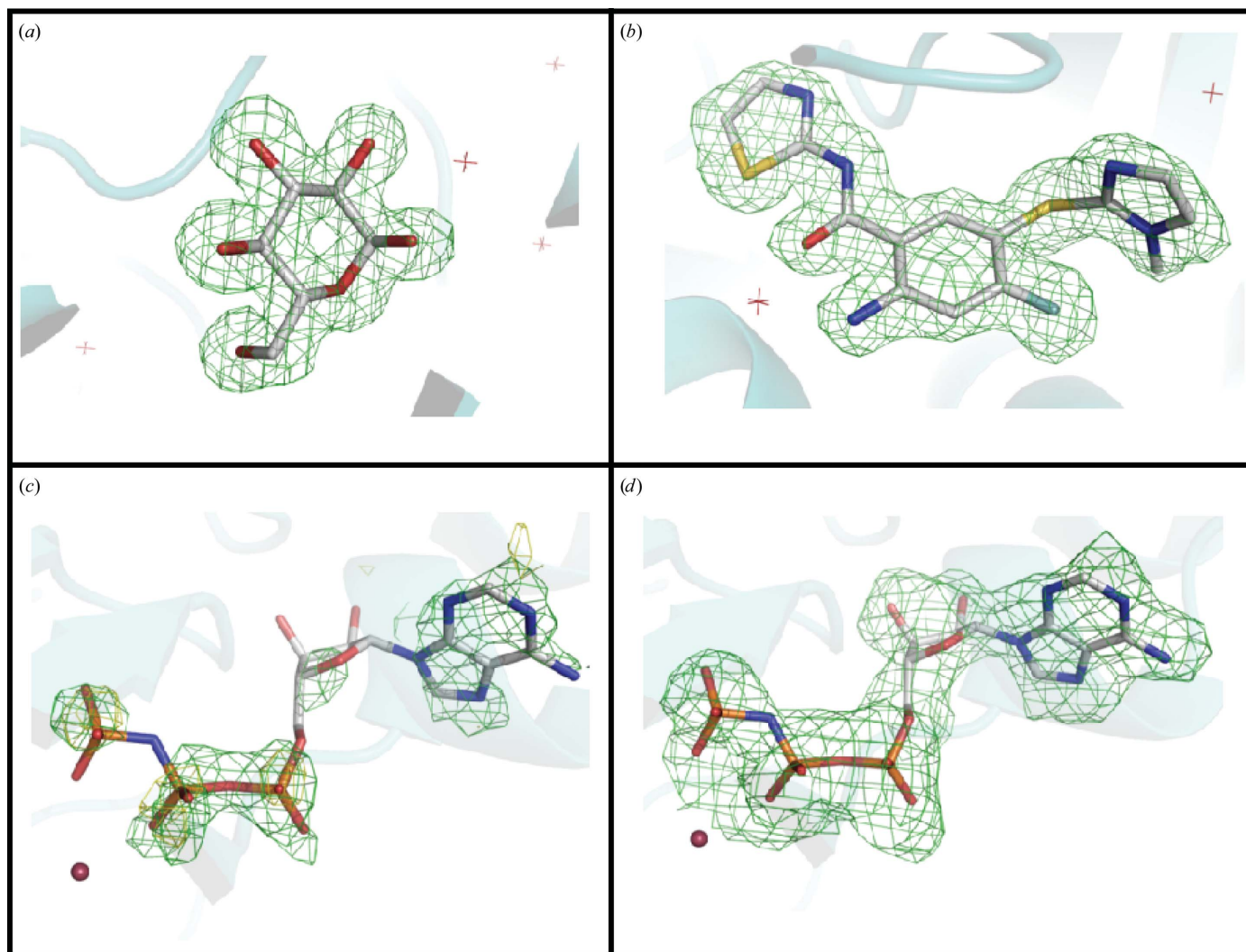

Figure 1
Simulated-annealing OMIT ($F_o - F_c$) maps contoured at 3σ for glucose (*a*) and TAFMT (*b*) in 3f9m. (*c*) Simulated-annealing OMIT ($F_o - F_c$) maps of the ATP pocket at 3σ: green contours are for the structure cocrystallized with AMP-PNP (3fgu) and yellow for that in its absence (3idh). (*d*) $F_o - F_c$ maps (3σ) from *BUSTER* refinement of the AMP-PNP-containing structure without adding AMP-PNP to the model used for refinement.

through the γ-phosphate of ATP before being trapped by Lys169. Indeed, Lys169 is ideally poised to act as the general acid catalyst that scavenges this proton once it is released after the formation of glucose 6-phosphate. The structure of the GK–glucose–AMP-PNP complex is in very good agreement with the theoretical model proposed by Zhang, Li *et al.* (2009) and supports the roles of Asp105 as the base catalyst and of Lys169 as the acid catalyst required for efficient catalysis of phosphoryl transfer between ATP and glucose. Models derived from the homologous structure of hexokinase 1 suggested the presence of an Mg^{2+} ion between the γ-phos-

phate, the glucose 6-hydroxyl and Asp205 (Mahalingam *et al.*, 1999).

Although the resolutions measured for the two AMP-PNP complexes (2.1 and 2.4 Å) and the atomic mass of Mg do not allow direct connection of the observed density to the nature of the bound atom, it seemed logical to attribute this density to Mg because (i) this density observed in the $F_o - F_c$ map (3σ) is located at an optimal position to form and stabilize the tertiary complex (GK–glucose–AMP-PNP) and (ii) only crystals of GK-glucose without bound AMP-PNP could be obtained in the absence of 1 mM magnesium chloride when crystallizing with 10 mM AMP-PNP in the drops. It is also worth noticing that the affinity of GK for ATP, and *a fortiori* for AMP-PNP, is poor beyond 10 mM (Molnes *et al.*, 2011).

It should be noted that while in some archaeal hexokinases (Mahalingam *et al.*, 1999) the Mg^{2+} is held in an octahedral coordination, in GK the Mg^{2+} is held in an hexahedral co-ordination and does not interact with the α-phosphate group (Fig. 4b). In GK, this single Mg^{2+} interacts directly with the side chain of Asp205 and with O1B, O2B and O3G of AMP-PNP, while the final two interactions with the side chains of Ser151 and Asp78 are mediated through two water molecules (W96 and W111). Amongst hexokinases, this mode of binding mediated by water molecules seems to be specific to GK. In the absence of AMP-PNP in the binary-complex structure (GK–glucose) weak density is still observed at a position close to the Mg atom and is maintained in GK–glucose–AMP-PNP complexes. This density was attributed to a water molecule as no Mg^{2+} was added to the crystallization conditions.

We can also rule out the existence of a 'noncatalytic ATP-binding site' in GK as observed in hexokinase I (Rosano *et al.*, 1999). Also, a twist of the β-phosphate to the protein surface after reaction has been proposed in the structure of a mutant monomeric hexokinase I (PDB entry 1dgk) where the phosphates were very close to the solvent (Aleshin *et al.*, 2000). This twist is unlikely in GK as it would imply a rearrangement
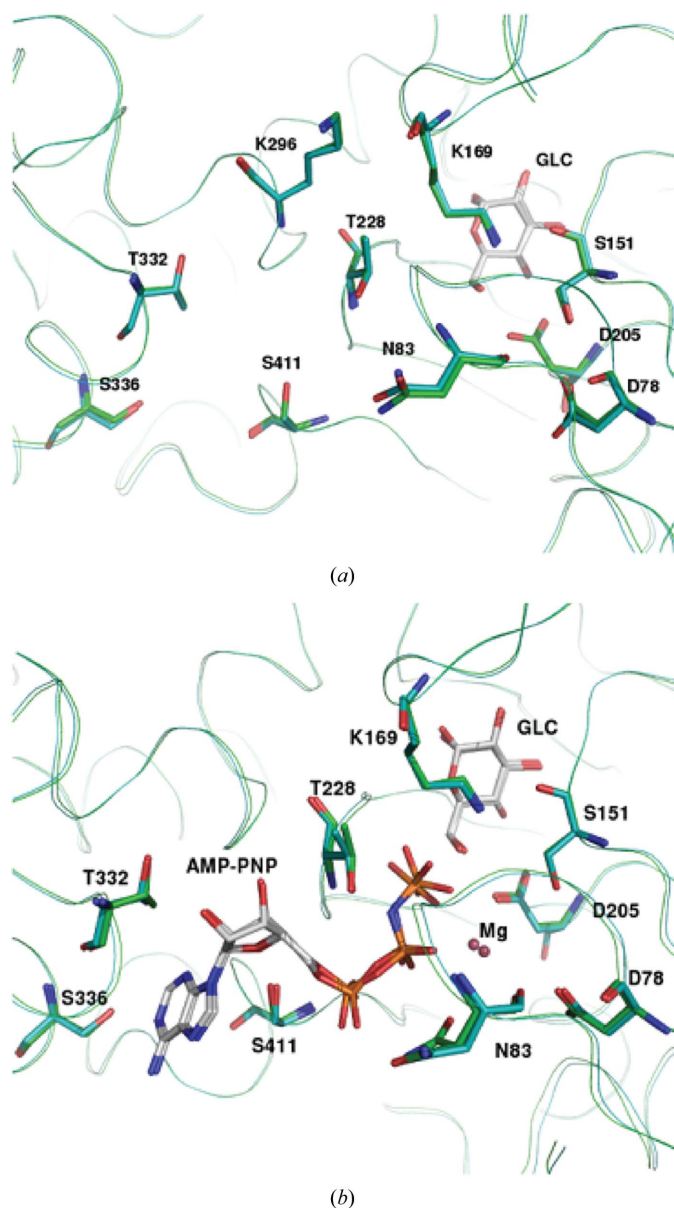

(a)

(b)

Figure 2
The positions of the active-site residues are not affected by the presence of TAFMT. (a) With bound glucose only in the presence (3f9m, green) or absence (3idh, blue) of bound TAFMT. (b) The same with bound glucose and AMP-PNP in the presence (3id8, green) or absence (3fgu, blue) of bound TAFMT.
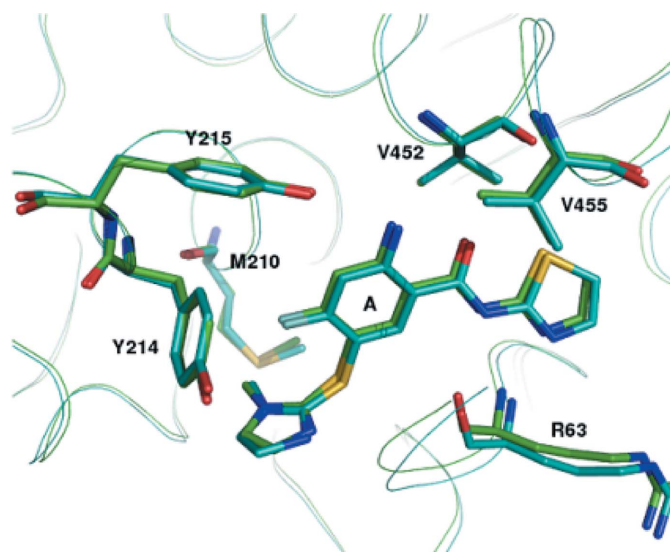

Figure 3
TAFMT binding. Position of TAFMT and neighbouring residues in the presence (3id8, blue) or absence (3f9m, green) of Mg AMP-PNP.

of the ADP molecule of about 3 Å after γ-phosphate transfer. Furthermore, a structure of the GK–glucose–ADP complex was also obtained in our laboratory (data not shown) which was very similar to the GK–glucose–AMP-PNP complex and showed no difference in pyrophosphate orientation.

3.3. The allosteric site flap is mobile

Despite a high overall similarity between our structures and 1v4s (or other structures from the Kamata group; Iino *et al.*, 2009; Kamata *et al.*, 2004; Mitsuya *et al.*, 2009; Nishimura *et al.*, 2009; Takahashi *et al.*, 2009), a difference was observed in the loop formed by residues 92–102. In our structures this loop does not show defined density despite the higher resolution than that of 1v4s, in which it was clearly observed. Indeed, in 1v4s this loop is stabilized because it participates in the crystal contacts. These contacts are absent in our space group and the

(a)

(b)

Figure 4
Structure of the active site of the ternary GK–glucose–AMP-PNP complex. (a) Asp205 and Lys169 are positioned to act as the general acid catalyst and the general base catalyst, respectively (PDB entry 3fgu; water molecules are represented by blue spheres and distances are represented as dotted lines). (b) Hexahedral Mg coordination in the GK active site.

loop is thus free to adopt a naturally poorly ordered structure. Several structures obtained with other proprietary activators also showed the same mobility leading to complete loss of electron density (not shown). Our conclusion is that this loop does not actively participate in the binding of these allosteric activators.

3.4. Other minor structural features

As a side issue, the resolution of 1.5 Å allowed the unambiguous confirmation of the absence of an S–S bridge in GK. Since the crystals were obtained in 100 m*M* glucose and showed only one binding site for glucose, we can also rule out the presence of another glucose-binding site, which had been suggested previously following experiments using fixation of a glucose analogue (Agius & Stubbs, 2000). We also observed a strong ion density (visible with $F_o - F_c$ up to 10σ) in the position where Kamata and coworkers reported a sodium ion in the structure 1v4s (Kamata *et al.*, 2004). Considering the intensity of the observed density and the absence of sodium ion in the buffer in our experiment, we labelled it as a potassium ion [occupancy = 1; B = 27 Å^2 (3id8) or 25 Å^2 (3fgu)].

4. Conclusion

In the present report, the active conformation of GK is described. As described in §3, these two GK structures are almost identical and can reasonably be considered to be the enzymatically 'active' conformation of GK. Our work also demonstrated that the binding of allosteric activators targeting the regulation site does not induce a specific 'super-active' conformation of GK. Thus, our structural work strongly supports the model in which activators work by specifically binding to closed 'active' GK, thus shifting the pre-existing glucose-dependent conformational equilibrium between open 'inactive' GK and closed 'active' GK toward the closed 'active' GK, as suggested by our previous kinetic study (Antoine *et al.*, 2009). As a consequence, activators may not be required to target the current activator site in order to stabilize the active conformation, as in theory it should be possible to target other regions of the GK hinge or regulatory helix 13 to hamper relaxation to the inactive state and thus increase GK activity. Nevertheless, as pointed out previously (Efanov *et al.*, 2005), considering the N-terminal position of the tissue-specific sequences of GK the development of tissue-specific GK activators will remain at best a challenging task. As part of the present study, the first structures of the binary complex of human GK bound to glucose and of the ternary complex of human GK bound to glucose and AMP-PNP have been solved.
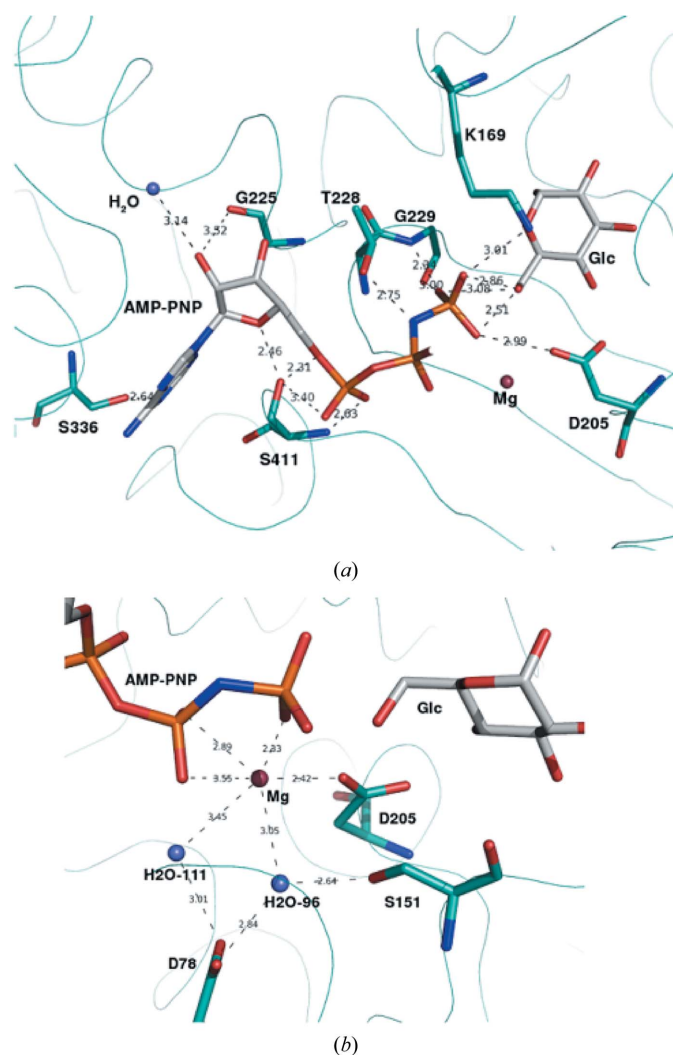
References

Agius, L. (2008). *Biochem. J.* **414**, 1–18.
Agius, L. & Stubbs, M. (2000). *Biochem. J.* **346**, 413–421.
Aleshin, A. E., Kirby, C., Liu, X., Bourenkov, G. P., Bartunik, H. D., Fromm, H. J. & Honzatko, R. B. (2000). *J. Mol. Biol.* **296**, 1001–1015.

Antoine, M., Boutin, J. A. & Ferry, G. (2009). *Biochemistry*, **48**, 5466–5482.

Bebernitz, G. R. *et al.* (2009). *J. Med. Chem.* **52**, 6142–6152.

Cuesta-Muñoz, A. L., Huopio, H., Otonkoski, T., Gomez-Zumaquero, J. M., Nänto-Salonen, K., Rahier, J., López-Enriquez, S., García-Gimeno, M. A., Sanz, P., Soriguer, F. C. & Laakso, M. (2004). *Diabetes*, **53**, 2164–2168.

Efanov, A. M., Barrett, D. G., Brenner, M. B., Briggs, S. L., Delaunois, A., Durbin, J. D., Giese, U., Guo, H., Radloff, M., Gil, G. S., Sewing, S., Wang, Y., Weichert, A., Zaliani, A. & Gromada, J. (2005). *Endocrinology*, **146**, 3696–3701.

Grimsby, J., Berthel, S. J. & Sarabu, R. (2008). *Curr. Top. Med. Chem.* **8**, 1524–1532.

Iino, T., Tsukahara, D., Kamata, K., Sasaki, K., Ohyama, S., Hosaka, H., Hasegawa, T., Chiba, M., Nagata, Y., Eiki, J. & Nishimura, T. (2009). *Bioorg. Med. Chem.* **17**, 2733–2743.

Johnson, L. N. (2009). *Q. Rev. Biophys.* **42**, 1–40.

Kabsch, W. (2010). *Acta Cryst.* D**66**, 125–132.

Kamata, K., Mitsuya, M., Nishimura, T., Eiki, J. & Nagata, Y. (2004). *Structure*, **12**, 429–438.

Lange, A. J., Xu, L. Z., Van Poelwijk, F., Lin, K., Granner, D. K. & Pilkis, S. J. (1991). *Biochem. J.* **277**, 159–163.

Larion, M., Salinas, R. K., Bruschweiler-Li, L., Brüschweiler, R. & Miller, B. G. (2010). *Biochemistry*, **49**, 7969–7971.

Mahalingam, B., Cuesta-Munoz, A., Davis, E. A., Matschinsky, F. M., Harrison, R. W. & Weber, I. T. (1999). *Diabetes*, **48**, 1698–1705.

Matschinsky, F. M. (1990). *Diabetes*, **39**, 647–652.

Matschinsky, F. M. (2009). *Nature Rev. Drug Discov.* **8**, 399–416.

Matschinsky, F. M., Zelent, B., Doliba, N. M., Kaestner, K. H., Vanderkooi, J. M., Grimsby, J., Berthel, S. J. & Sarabu, R. (2011). *Handb. Exp. Pharmacol.*, pp. 357–401.

Mitsuya, M., Kamata, K., Bamba, M., Watanabe, H., Sasaki, Y., Sasaki, K., Ohyama, S., Hosaka, H., Nagata, Y., Eiki, J. & Nishimura, T. (2009). *Bioorg. Med. Chem. Lett.* **19**, 2718–2721.

Molnes, J., Teigen, K., Aukrust, I., Bjørkhaug, L., Søvik, O., Flatmark, T. & Njølstad, P. R. (2011). *FEBS J.* **278**, 2372–2386.

Murshudov, G. N., Skubák, P., Lebedev, A. A., Pannu, N. S., Steiner, R. A., Nicholls, R. A., Winn, M. D., Long, F. & Vagin, A. A. (2011). *Acta Cryst.* D**67**, 355–367.

Nishimura, T., Iino, T., Mitsuya, M., Bamba, M., Watanabe, H., Tsukahara, D., Kamata, K., Sasaki, K., Ohyama, S., Hosaka, H., Futamura, M., Nagata, Y. & Eiki, J. (2009). *Bioorg. Med. Chem. Lett.* **19**, 1357–1360.

Painter, J. & Merritt, E. A. (2006). *Acta Cryst.* D**62**, 439–450.

Perrakis, A., Harkiolaki, M., Wilson, K. S. & Lamzin, V. S. (2001). *Acta Cryst.* D**57**, 1445–1450.

Polakof, S. (2010). *Recent Pat. DNA Gene. Seq.* **4**, 1–9.

Rosano, C., Sabini, E., Rizzi, M., Deriu, D., Murshudov, G., Bianchi, M., Serafini, G., Magnani, M. & Bolognesi, M. (1999). *Structure*, **7**, 1427–1437.

Takahashi, K., Hashimoto, N., Nakama, C., Kamata, K., Sasaki, K., Yoshimoto, R., Ohyama, S., Hosaka, H., Maruki, H., Nagata, Y., Eiki, J. & Nishimura, T. (2009). *Bioorg. Med. Chem.* **17**, 7042–7051.

Vagin, A. & Teplyakov, A. (2010). *Acta Cryst.* D**66**, 22–25.

Vionnet, N., Stoffel, M., Takeda, J., Yasuda, K., Bell, G. I., Zouali, H., Lesage, S., Velho, G., Iris, F., Passa, P., Froguel, P. & Cohen, D. (1992). *Nature (London)*, **356**, 721–722.

Zhang, J., Li, C., Shi, T., Chen, K., Shen, X. & Jiang, H. (2009). *PLoS One*, **4**, e6304.

Zhang, J., Yang, P. L. & Gray, N. S. (2009). *Nature Rev. Cancer*, **9**, 28–39.